Magnetic-field effects in energy relaxation mediated by Kondo impurities in mesoscopic wires

G. Göppert,[1] Y. M. Galperin,[2] B. L. Altshuler,[1,3] and H. Grabert[4]

[1]*Physics Department, Princeton University, Princeton, New Jersey 08544*
[2]*Department of Physics, University of Oslo, P.O. Box 1048, N-0316 Oslo, Norway*
and Argonne National Laboratory, 9700 S. Cass Avenue, Argonne, Illinois 6043
[3]*NEC Research Institute, 4 Independence Way, Princeton, New Jersey 08540*
[4]*Fakultät für Physik, Albert-Ludwigs-Universität, Hermann-Herder-Straße 3, D 79104 Freiburg, Germany*

We study the energy distribution function of quasiparticles in short voltage biased mesoscopic wires in the presence of magnetic impurities and applied magnetic field. The system is described by a Boltzmann equation where the collision integral is determined by coupling to spin-$\frac{1}{2}$ impurities. We develop a theory of the coupling of nonequilibrium electrons to dissipative spins. This theory is valid as long as the characteristic smearing of the steps in the energy distribution function, which depends both on the bias voltage and the location of the probe, exceeds the Kondo temperature. We further address the renormalization of coupling constants by nonequilibrium electrons. Magnetic-field dependence of the energy relaxation rate turns out to be nonmonotonic. For low magnetic field an enhancement of energy relaxation is found, whereas for larger magnetic fields the energy relaxation decreases again meeting qualitatively the experimental findings by Anthore *et al.* (cond-mat/0109297). This gives a strong indication that magnetic impurities are in fact responsible for the enhanced energy relaxation in copper wires. Our theoretical results are in good agreement with the experiment at large bias voltages where the theory is applicable. At the same time, at small bias voltages there are substantial quantitative deviations. Furthermore, the concentration of the spins, which follows from the energy relaxation for Cu, seems to to be substantially higher than the concentration estimated from weak localization (dephasing rate) measurements. Since the approach presented is valid only above Kondo temperature, it does not apply to the related problem of weak localization at low temperature in equilibrium.

I. MOTIVATION AND OVERVIEW

Energy relaxation of "hot" electrons in disordered conductors at low enough energies was for a long time believed to be determined by direct interaction between electrons. Recent experiments on mesoscopic wires (see Ref. 1, and references therein) have shown that Kondo impurities (localized spins) lead to much higher energy relaxation rates than those predicted by the standard theory.[2]

On the other hand, the inelastic collisions of electrons and their spin flips are directly related to the phase coherence time probed by weak localization effects, such as low-field magnetoresistance. The problem of decoherence in weak localization was recently revisited and intensively discussed.[1,3,4]

Theoretical studies by various groups [5–10] lead to a satisfactory and consistent explanation of energy relaxation experiments by Kondo impurity mediated electron-electron interaction in the gold wires by Pierre *et al.*[1] Those gold wires were contaminated by iron impurities, and the concentration of the impurities could be independently estimated from the magnetoresistance as well as from the temperature dependence of the resistivity. As a result, it was possible to carry out a parameter-free comparison of theory and experiment.[7–9]

At the same time the copper samples in the first energy relaxation experiment by Pothier *et al.*[11] were fitted using concentration and Kondo temperature of the paramagnetic impurities as free parameters. The parameters obtained from energy relaxation disagree with those obtained from the magnetoresistance experiments of the same sample.[12,13] Therefore, whether or not magnetic impurities are responsible for these effects is dubious.

Since the behavior of magnetic impurities is sensitive to the applied magnetic field, studies of energy relaxation in the presence of the magnetic field could either rule out or validate magnetic impurities as a relevant scattering process in energy relaxation. Recently, Anthore *et al.*[14] reported results of such experiments in Cu wires that indicate a strong dependence of the energy relaxation on the magnetic field suggesting that magnetic impurities indeed play a role for the copper wires as well.

In this paper we perform a theoretical study of transport and energy relaxation in a mesoscopic wire in dependence on an applied magnetic field. We use a diffusive Boltzmann equation to account for the static scatterers and focus in the inelastic collision integral on magnetic impurities. The findings are in qualitative agreement with the experimental data in Ref. 14 supporting the presumption that scattering with magnetic impurities is the essential mechanism of energy transfer at low temperatures. However, the apparent inconsistency between the values of the experimentally observed energy relaxation rate and the dephasing rate extracted from the magnetoresistance in Cu wires remains puzzling.

Starting with a brief discussion of the experiment we propose in Sec. II a simple physical picture to explain the anomalous dependence of the energy relaxation on the magnetic field. In Sec. III follows a theoretical description in terms of a renormalized Hamiltonian restricting the interaction processes to the coupling to electron-hole pairs only. We

then present in Sec. IV the numerical procedure and the comparison with experimental results. Section V is devoted to a discussion of the interpretation and validity of the approach as well as its possible extensions.

II. EXPERIMENTAL SITUATION AND PHYSICAL PICTURE

Here, we briefly describe the experimental situation in Ref. 14 and a possible qualitative explanation of their findings.

The experimental setup in Ref. 14 consists of a thin copper wire of about 45 nm thickness, 105 nm width, and 5 μm length connected to two metallic leads. The leads are biased by an external voltage source $U = 0.1$ mV and $U = 0.3$ mV imposing a steady-state current through the wire. The setup is placed in a dilution refrigerator with a temperature of 25 mK and a magnetic field up to 2.2 T is applied. The elastic mean free path can be estimated to be much smaller than the length of the wire, L, so that the transport of electrons between the contacts is diffusive. The diffusion constant $D = 90$ cm^2/s, estimated from the low-temperature resistance, leads to a diffusion time of $\tau_D = L^2/D = 2.8$ ns.

The aim of the experiment was to study energy distribution of electrons. The distribution function was determined by tunneling to an underlying aluminum probe electrode. The differential tunneling conductance is given by a convolution over the electron distribution functions in the wire and in the probe electrode, both for $B = 0$ and $B \neq 0$, compare with Refs. 11, 15 and 14, respectively. In the case of vanishing magnetic field, the aluminum probe electrode is in the superconducting state, and the peaked density of states of the probe electrode allows one to straightforwardly extract the energy distribution in the wire from the I-V characteristic of the junction.

For finite magnetic fields, however, the aluminum probe electrode is in the normal state. In this case the deconvolution has been made using a zero bias anomaly. Unfortunately, the latter procedure is less accurate. Considering the numerical transformation depicted in Fig. 2 of Ref. 14, we expect that the strongest variations due to uncertainties in the shape and the depth of the zero bias anomaly arise at the "Fermi points" $\epsilon = \pm eU/2$. Furthermore, the tunnel probe experiment in equilibrium, $U \to 0$, gave the temperature of 65 mK, which differs from the actual refrigerator temperature. This might be due to an oversimplification of the environmental impedance responsible for the zero bias anomaly.[14] Consequently, the resulting distribution function has to be taken with some care; in particular, near the Fermi points.

The electron distribution function in the absence of inelastic scattering is just a linear combination of the distributions in the left and right electrode,[16]

$$f_0(\epsilon, x) = (1-x)f_F(\epsilon - eU/2) + xf_F(\epsilon + eU/2). \quad (1)$$

Here, $f_F(\epsilon)$ is the Fermi function while x is the longitudinal coordinate of the observation point in units of the total length L. At low temperatures, the distribution (1) has steps in both ϵ and x dependences. These steps are smeared by inelastic processes, such as electron-phonon and electron-electron in-

teraction. As a result, the distribution in the middle of the wire turns out to be almost insensitive to the bath temperature.[17,18] The smearing depends on the effective inelastic relaxation time, and the latter can be estimated from the experimentally observed distribution function.

The first experiments[11,15] for $B = 0$ have clearly shown that the smearing is too strong to be attributed to the electron-electron or electron-phonon interaction. Therefore, in the following we do not take these interactions into account.

The qualitative outcome of the experiment[14] is that the behavior of the inelastic relaxation rate is a nonmonotonic function of the magnetic field B. For $B \lesssim B_1 = eU/4.3\mu_B$, the relaxation rate *increases* with magnetic field and reaches a maximum at $B \approx B_1$. At stronger fields, $B > B_1$, it decreases with further increasing magnetic field, and at $B \approx B_2 = eU/2\mu_B$ it reaches almost the same value as it had at $B = 0$ and then decreases further.

The explanation of such a complex behavior given in Ref. 14 is based on electron scattering by magnetic impurities. For vanishing magnetic field, the spin system is degenerate and only second- or higher-order scattering processes contribute to energy relaxation. For finite magnetic fields, there exists also a first-order contribution with energy $E_H = g\mu_B B$ (equal to the Zeeman splitting) transferred to or from the spin system. Therefore, the energy relaxation rate increases. However, for $E_H > eU$ the spins are completely polarized and can no longer contribute to energy relaxation. Consequently, again only higher-order processes are effective. Comparing this explanation with the experiment, one estimates the gyromagnetic factor for the impurity spins as $g \approx 2$.

Thus, electron-spin interaction taken into account in the lowest order of the perturbation theory explains, in principle, the main experimental features. However, from the theoretical point of view, there appears a subtlety. The problem is that the higher-order terms, estimated within the framework of the t-matrix approach in Refs. 6,7,10, lead to a divergent contribution $\sim J^4/(\epsilon \mp E_H)^2$ to be integrated over. Here J is the renormalized coupling constant that defines the strength of the electron-impurity interaction. The suggestion[6,8,9] to introduce a cutoff at the Korringa width,[19] $K \sim J^2$ gives a result that is comparable with the first-order contribution. Consequently, there is no systematic expansion in powers of the coupling constant, and one needs a generalized approach that is not based on expansion in terms of the interaction strength.

The aim of the present paper is to develop an approach capable of treating lowest- and higher-order contributions within a unified scheme. We show that the problem can be described as electrons coupled to a dissipative spin system. The dissipation of impurity spins is, in turn, caused by creation/annihilation of electron-hole pairs due to electron-spin coupling. We show that this scheme includes the divergent higher-order contributions appearing in the t-matrix approach. Using our approach, we derive an electron-spin collision integral expressed through spin-spin correlation functions. An important feature of these correlation functions is that their dependence on the electron energy is automatically broadened by Korringa-type processes. These pro-

cesses, however, depend on the actual electron distribution rather than on the thermal equilibrium distribution as in Ref. 19. As a result, the applied voltage plays the role of an effective temperature.

The crucial difference between the cases $B=0$ and $B \neq 0$ is the following. At zero magnetic field, all spin-spin correlation functions are centered at zero energy and behave as $K/(\epsilon^2+K^2)$. It is important that in the collision integral these correlators are multiplied by a combination of the electron distribution functions, which at small energies is proportional to ϵ. Consequently, the broadening turns out to be unimportant,[7] and one can omit K^2 in the denominator. This way the resulting collision integral becomes proportional to J^4 and one recovers the results[6,7] of the t-matrix approach.

At finite magnetic fields, however, the spin-spin correlation function decomposes into three contributions. The non-spin-flip part is still centered at zero energy, while the two spin-flip contributions are peaked at $\epsilon=\pm E_H$. Let us, for a moment, accept the above simplified form of the correlation function and assume $K\to 0$. Since in this case $K/[(\epsilon \mp E_H)^2+K^2]\to\pi\delta(\epsilon\mp E_H)$, the two spin-flip correlation functions with finite-energy transfer lead indeed to the desired first order in J^2 contribution. In this simplified case only the non-spin-flip correlation function contributes to the order J^4 in the collision integral.

Using the t-matrix approach with a finite cutoff K, introduced by hand, would lead to a double counting of the first order in J^2 contribution. Here, on the other hand, the cutoff is included automatically and the first order is accounted for correctly.

In this simplified case the reasoning to explain the experimental data follows the lines of the experimentalists. The only difference is that for $E_H>eU$, where the spin-flip contribution is already frozen out, there remains just 1/3 of the $B=0$ energy relaxation because only the non-spin-flip component contributes to energy relaxation in order J^4. In practice, K is not constant but depends on frequency. Therefore, the correlation functions are not Lorentzian shaped and the spin-flip terms will also contribute to the J^4 term. Further, the width decreases with increasing magnetic field for the non-spin-flip component and therefore energy relaxation mediated by magnetic impurities dies out for $E_H\gg eU$.

We believe that our approach provides a consistent explanation of the magnetic-field dependence of the nonequilibrium electron distribution in diffusive wires with magnetic impurities.

III. THEORETICAL DESCRIPTION

Here we present a simplified version of the theory with isotropically renormalized coupling constant J independent of energy. In general, the renormalization can be anisotropic and energy dependent. These generalizations, which do not alter the underlying physics, are discussed in appendixes.

We assume that the metallic wire is in the diffusive limit, i.e., the elastic relaxation time is much smaller than other time scales. We also assume that the distribution function of electrons does not depend on the spin. The energy distribution of the electrons is governed by the Boltzmann equation,

$$\frac{\partial f(\epsilon,x)}{\partial t}-\frac{1}{\tau_D}\frac{\partial^2 f(\epsilon,x)}{\partial x^2}+I\{f\}=0, \tag{2}$$

$$I\{f\}=\int d\omega\{f(\epsilon)[1-f(\epsilon-\omega)]W(\epsilon,\omega)$$
$$-[1-f(\epsilon)]f(\epsilon-\omega)W(\epsilon-\omega,-\omega)\}. \tag{3}$$

Here, we include the density of states ρ in the scattering rate $W(\epsilon,\omega)$ and omit for convenience the explicit spatial dependence of the distribution function. The rate W describes the transitions between two electron states with energies ϵ and $\epsilon-\omega$ mediated by coupling to the dissipative spin system. Its explicit form is given by

$$W(\epsilon,\omega)=(c_{\mathrm{imp}}/\rho\hbar)[\rho J/2]^2 C(\omega), \tag{4}$$

where c_{imp} is the impurity density. The explicit dependence of W on electron energy ϵ is taken into account in the concrete calculations. However, it is not important for the present discussion. Further, $C(\omega)$ is the Fourier transform of a spin-spin correlation function. The latter can be split as

$$C(t)=[C_+(t)+C_-(t)]/2+C_z(t), \tag{5}$$

where

$$C_\pm(t)=\langle S^\pm(t)S^\mp(0)\rangle, \quad C_z(t)=\langle S^z(t)S^z(0)\rangle. \tag{6}$$

The averages here mean the spin and electron trace weighted with the unknown nonequilibrium density. The time evolution is governed by the Hamiltonian $H=H_0+H_I$, where

$$H_0=\sum_{k\sigma}\epsilon_{k\sigma}C_{k\sigma}^\dagger C_{k\sigma}-E_H S^z \tag{7}$$

describes free electrons. Here, operators $C_{k\sigma}^\dagger$ and $C_{k\sigma}$ create and annihilate an electron in a given orbital k and spin σ state. $\epsilon_{k\sigma}$ is the energy of this state. The second term in Eq. (7) describes a spin-$\frac{1}{2}$ impurity with Zeeman splitting $E_H=g\mu_B B$. The interaction Hamiltonian

$$H_I=J\sum_{kk'\sigma\sigma'}\mathbf{S}\cdot\mathbf{s}_{\sigma'\sigma}C_{k'\sigma'}^\dagger C_{k\sigma} \tag{8}$$

couples electrons to the impurity spin system via the renormalized coupling strength J, rather than the bare one, J_0. Further, the electron is coupled only to one impurity spin since we assume that the impurity density c_{imp} is small enough to neglect higher-order terms.

Using this renormalized Hamiltonian we will restrict our calculation for the time evolution of $C(t)$ to the coupling to simple electron-hole pair excitations only, see Appendix A for details. A similar procedure was already used in Ref. 20 to discuss the impurity spin resonance linewidth in equilibrium using Baym and Kadanoff's kinetic equations. Here, the spin-spin correlation functions are calculated using the conventional projection operator technique.[21] The results read

$$C_z(\omega) = \frac{1}{2} \frac{\nu_z(\omega)}{\omega^2 + \nu_z(\omega)^2}, \tag{9}$$

$$C_\pm(\omega) = \frac{2\mathcal{P}_\pm \nu_\pm(\omega)}{[\omega \mp E_H]^2 + \nu_\pm(\omega)^2}. \tag{10}$$

The functions $\nu_z, \nu_\pm$ describing damping of spin fluctuations can be expressed through an auxiliary function

$$\zeta(\omega) = \int d\epsilon' f(\epsilon')[1 - f(\omega + \epsilon')] \tag{11}$$

stemming from the coupling to electron-hole pairs. They read

$$\nu_z(\omega) = \pi(\rho J)^2[\mathcal{P}_+ \zeta(\omega - E_H) + \mathcal{P}_- \zeta(\omega + E_H)], \tag{12}$$

$$\nu_\pm(\omega) = (\pi/4)(\rho J)^2[2\zeta(\omega \mp E_H) + \zeta(\omega)/\mathcal{P}_\pm]. \tag{13}$$

Further, $\mathcal{P}_\pm$ is the occupation probability for impurity spin up or down, respectively. These probabilities are determined by a master equation

$$d\mathcal{P}_\pm/dt = -\Gamma_\pm \mathcal{P}_\pm + \Gamma_\mp \mathcal{P}_\mp, \quad \mathcal{P}_+ + \mathcal{P}_- = 1, \tag{14}$$

which can be solved in the steady state leading to

$$\mathcal{P}_\pm = \Gamma_\mp/(\Gamma_+ + \Gamma_-). \tag{15}$$

Here, the inverse lifetime for the spin-up (down) state, $\Gamma_\pm$, is determined by the expression

$$\Gamma_\pm = \frac{(\rho J)^2}{4\hbar \mathcal{P}_\pm} \int d\omega \zeta(-\omega) C_\pm(\omega). \tag{16}$$

For a given electron distribution, the set of Eqs. (15) and (16) determines the occupation probabilities of the spin system. From Eqs. (5) and (6) one can prove the sum rule for the correlation function,

$$C(t=0) = \int (d\omega/2\pi) C(\omega) = 3/4 = S(S+1), \tag{17}$$

which is independent of magnetic field. In the weak-coupling limit

$$C_\pm(\omega) = 2\pi \mathcal{P}_\pm \delta(\omega \mp E_H), \quad C_z(\omega) = \pi\delta(\omega)/2. \tag{18}$$

Inserting this result into the rates (4) and (16), we recover the Fermi's golden rule expressions for the electron collision operator for the case of interaction with a single spin. Here the δ functions signalize energy conservation. The dissipation leads to an energy uncertainty that, in turn, results in a broadening of the δ functions. The final result differs from that obtained by the t-matrix approach[22] by allowing for a finite-energy uncertainty.

For vanishing magnetic field, $E_H = 0$, the occupation numbers $\mathcal{P}_\pm = 1/2$, and the correlation function simply reads $C(\omega) = 3C_z(\omega)$. Inserted in the collision integral, our expression with the renormalized coupling constant J from Eq. (B6) is consistent with the results of Refs. 6 and 7. The advantage here is that the cutoff $\nu_z(0) = \pi(\rho J)^2\zeta(0)$, sug-

gested in Refs. 6,8,9, is naturally included. This cutoff equals the Korringa width K. For weak coupling only elastic scattering survives and we get $W(\epsilon) = \tau_{sf}^{-1}\delta(\epsilon)$ where the time τ_{sf} is usually referred to as spin-flip time.[23] In this case the collision integral vanishes identically and one has to go beyond the lowest order.

Further, our expression for the correlation function in equilibrium and vanishing magnetic field coincides with the results of Wöger and Zittartz[24] based on a Nagaoka-like decoupling scheme. Using Suhl's t matrix for the renormalized coupling constants, the spin susceptibilities follow from proper kinetic equations. The procedure is actually similar to the one used in Ref. 20 for the analysis of the impurity spin resonance linewidth.

An asymmetric rate $W(\omega)$ in the collision integral (3) in general does not allow for a thermalized solution. However, this is one of the basic requirements the Boltzmann equation has to fulfill. In order to show that our specific rate allows for such a solution, we expand $W(\omega)$ in powers of J^2. In the collision integral we get higher orders in the distribution function, however, with a symmetric kernel. For the C_z term this is obviously $1/\omega^{2n}$. In contrast, the $C_\pm$ kernel is given by $1/(\omega \mp E_H)^{2n}$ that has to be summed over $\pm$ to lead to an even expression in ω. Taking the logarithm of the integrand leads to the usual condition $\ln(f/1-f) = $ const solved by the Fermi distribution proving the statement. Since the effective electron temperature profile $T_{el}(x)$ in a sufficiently long wire in the diffusive limit depends only on the diffusive motion of the electrons in the wire[17] the Boltzmann equation (2) will eventually lead to the correct thermalized distribution covering the so-called "hot electron" limit.

IV. NUMERICAL PROCEDURE AND COMPARISON WITH EXPERIMENT

For the numerical procedure we use anisotropic and energy-dependent coupling constants $J_\pm^z(\epsilon)$ and $J^\pm(\epsilon)$ given in Appendix B, Eqs. (B6) and (B7), respectively. They have to be calculated self-consistently as functionals of the final nonequilibrium distribution function. This procedure leads to a slight complication of the formulas in the preceding section but does not alter their structure. The detailed changes to be made are listed in Appendix D.

We have started with the solution (1) of the impurity-free problem inserted in Eqs. (B6) and (B7) for the coupling constants, Eqs. (D5) and (D6) for the auxiliary functions $\zeta_z(\omega)$ and $\zeta_\pm(\omega)$, and Eq. (3) for the collision integral. Then the distribution function was evolved iteratively using the Boltzmann equation (2) with collision operator (3). At each iteration both the coupling constants and the correlation functions were updated. After about 120 iterations a stationary solution has been reached.

To make an independent comparison of the finite field data, we have fitted the impurity density with data at $B = 0$. The resulting impurity concentration $c_{imp} = 8$ ppm is in accordance with the experimental purity of copper of 99.999%.[14] The density of states is chosen to be $\rho = 0.21/(\text{site eV})$.[25] The Kondo temperature, not known so far, has been assumed as $T_K = 0.4$ K. Further, the gyromag-
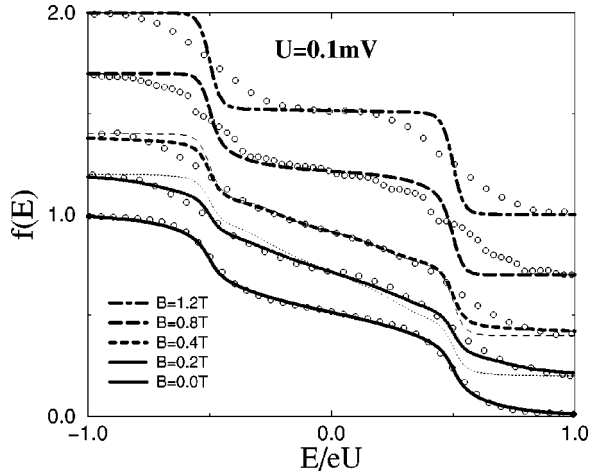
FIG. 1. Comparison of experimentally determined distribution functions from Ref. 14 (symbols) with the theoretical predictions for various magnetic fields and $U=0.1$ mV. The thick lines are data gained from solving the Boltzmann equation where the impurity spins are out of equilibrium, whereas the thin ones (differing from the thick lines for two values of B only) are determined with impurity spins fixed to equilibrium. The distribution functions are given from bottom to top for $B=0.0,0.2,0.4,0.8,1.2$ T and shifted vertically by steps of 0.2 and 0.3, respectively.

netic factor was chosen as $g\approx2$, see the review of experimental results in Sec. II.

The comparison of the distribution functions for $U=0.1$ mV is shown in Fig. 1 and for $U=0.3$ mV in Fig. 2. The symbols are the distribution functions for several magnetic fields obtained from experimental data by a deconvolution procedure. Note that a magnetic field of $B=1$ T leads to a Zeeman splitting $E_H\approx0.12$ meV. Thick lines are the
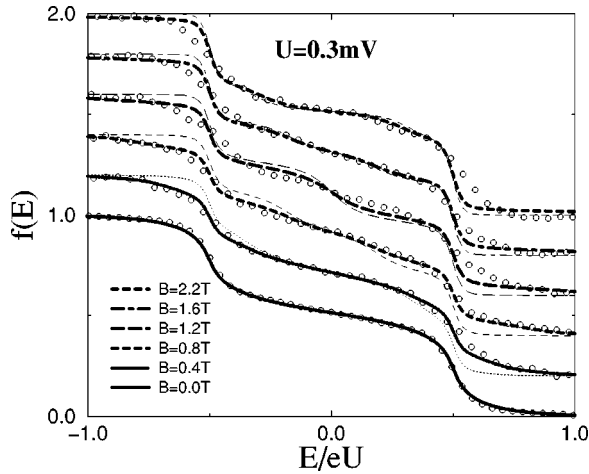

FIG. 2. Comparison of experimentally determined distribution functions from Ref. 14 (symbols) with the theoretical predictions for various magnetic fields and $U=0.3$ mV. The thick lines are data gained from solving the Boltzmann equation where the impurity spins are out of equilibrium, whereas the thin ones are determined with impurity spins fixed to equilibrium. The distribution functions are given from bottom to top for $B=0.0,0.4,0.8,1.2,1.6,2.2$ T and shifted vertically by steps of 0.2.

outcome of our numerical procedure allowing for the nonequilibrium occupation numbers (15) for the impurity spins. For comparison, thin broken lines are the results obtained from the Boltzmann equation for equilibrium impurity spins. It is clear that the results for relatively weak magnetic fields, $E_H<eU$, agree with theoretical predictions only if the nonequilibrium spin population is taken into account. Consequently, we conclude that the impurity states are indeed *out of equilibrium*. Since the only spin-relaxation mechanism taken onto account is an interaction with electrons, it follows that "hot" impurity centers serve as *mediators* for the electron-electron interaction.

In large magnetic fields, $E_H>eU$, according to the theory, the impurity-induced energy relaxation is frozen out. Consequently, to obtain a quantitative agreement with the experimental results shown in Fig. 1 one should take into account other, though weak, scattering mechanisms.

Further, we observe that the numerical data for $U=0.3$ mV and $B=1.2$ T show an additional step in the middle of the energy distribution function. This can be explained in terms of the lowest-order, J^2, scattering with impurity spins where the transferred energy between electron and impurity spin is always $\pm E_H$. The origin is that the Zeeman splitting E_H at this magnetic field is almost $eU/2$. Electrons in the energy region slightly below $-eU/2$ are scattered slightly below $\epsilon=0$ because the distribution function differs strongly in these two regions. The same statement is correct for electrons that scatter from slightly above $\epsilon=0$ to slightly above $eU/2$. Scattering between other regions is suppressed by the small difference in the distribution function at the contributing regions. Using only the first order in J^2 description for energy relaxation, this feature would be much more pronounced as the one shown in Fig. 2. The finite width in the correlation functions (10) responsible for these inelastic processes smear already out most of the sharp features. We assume that additional energy relaxation processes, such as the direct electron-electron interaction are responsible for the missing step in the corresponding experimental data. This feature is therefore assumed to be an artifact of our numerical calculation caused by neglecting other scattering mechanisms.

Since, in our theoretical approach, additional scattering mechanisms that lead to small energy transfer are missing and further the experimental data uncertainties are most pronounced at the "Fermi points" $\epsilon=\pm eU/2$, it is not reasonable to consider these energy regions in more detail. To characterize the quality of our fits we focus the comparison between our numerical data and the experiment to the "plateau" region around $\epsilon\approx0$ in the middle of the two-step distribution function. The negative slope of the distribution function is a good indicator of the energy relaxation strength as long as it is small. For vanishing energy relaxation it is zero and it increases with increasing energy relaxation. In Fig. 3 we show the averaged negative slope of the energy distribution functions at the plateau near $\epsilon\approx0$ in dependence of the magnetic field B. We find that the theoretical data (solid lines) meet the qualitative outcome in Sec. II of increasing energy relaxation up to the maximum value at about $E_H\approx eU/2$ and then decreasing again, showing at $E_H\approx eU$

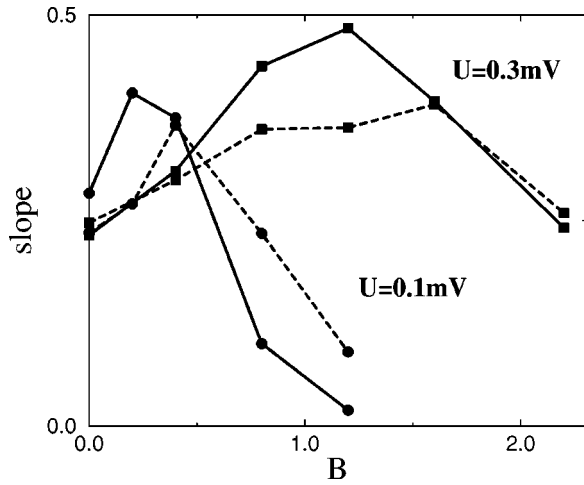FIG. 3. Averaged negative slope of the energy distribution functions at the plateau near $\epsilon \approx 0$ in dependence of the magnetic field B in units of Tesla. The data for $U = 0.1$ mV (dots) are extracted from Fig. 1 and for $U = 0.3$ mV (squares) from Fig. 2. The solid lines are our numerical data and the dashed lines the experimental ones.

about the same value as at $E_H = 0$. The data, however, cannot explain the experimental outcome (dashed lines) in quantitative detail, which is not further surprising taking into account the simplifications we made.

V. DISCUSSION

Let us first discuss the outcome of our findings in terms of an inelastic relaxation rate, then focus on the justification of various assumptions including the discussion of the Kondo temperature not addressed in previous sections, and conclude with an outlook to further work.

A. Inelastic relaxation rate

Since the distribution functions of electrons and spins are out of equilibrium, the inelastic relaxation cannot, in general, be discussed in terms of a single relaxation rate. In the following we use two quantities to describe the inelastic relaxation.

First, we consider the collision integral (3) in relaxation time approximation. We find the corresponding rate to be

$$\frac{1}{\tau_{\rm rt}} \equiv \int d\epsilon' W(\epsilon')[1 - f(\epsilon - \epsilon') + f(\epsilon + \epsilon')]$$

$$= \frac{1}{\tau_{\rm sf}} - \int d\epsilon' f(\epsilon - \epsilon')[W(\epsilon') - W(-\epsilon')], \quad (19)$$

with the spin-flip time defined by the exact relation following from the sum rule (17) for the correlation function, $C(\omega)$,

$$\int d\epsilon W(\epsilon) = \frac{\pi}{2\hbar} \frac{c_{\rm imp}}{\rho} S(S+1)(\rho J)^2 \equiv \frac{1}{\tau_{\rm sf}}. \quad (20)$$

Here, for simplicity, we consider again an energy independent and isotropic coupling constant J leading to $W(\epsilon, \omega) = W(\omega)$. The inverse relaxation time $1/\tau_{\rm rt}$ equals the imagi-

nary part of the electron self-energy considering only interaction with localized impurity spins. To discuss this expression at finite magnetic fields, we approximate $W(\epsilon)$ by its weak-coupling form to get

$$\frac{1}{\tau_{\rm rt}} = \frac{1}{\tau_{\rm sf}} \left\{ 1 - \frac{2}{3} [f(\epsilon - E_H) - f(\epsilon + E_H)](\mathcal{P}_+ - \mathcal{P}_-) \right\}, \quad (21)$$

where $(\mathcal{P}_+ - \mathcal{P}_-)$ is the mean polarization of the localized spin, see Eqs. (14) and (15). For monotonic distribution functions, the additional term leads to a nonpositive contribution and we have always $1/\tau_{\rm rt} \leq 1/\tau_{\rm sf}$. At small magnetic fields the combination of occupation numbers and distribution functions in Eq. (21) decreases and becomes of order $(E_H/eU)^2$. In equilibrium we find this contribution to be $\sim \tanh^2(\beta E_H/2)$, which leads to an exact cancellation of the spin-flip term, $1/\tau_{\rm rt} = 1/3\tau_{\rm sf}$, for large magnetic fields, $E_H \gg k_B T$. This is in accordance with the fact that for large magnetic fields the spin-flip contribution is completely frozen out. Out of equilibrium, the contribution stemming from the distribution functions behaves similarly and cannot explain the increase of energy relaxation for small magnetic fields.

Whereas in the collision operator (3) small-energy transfer is canceled by the distribution functions, the relaxation rate in Eq. (19) includes terms stemming from elastic scattering for $\epsilon' = 0$. To consider the pure inelastic part, we define an inelastic scattering rate by

$$\frac{1}{\tau_{\rm in}} \equiv \frac{1}{\tau_{\rm rt}} - \frac{1}{\tau_{\rm el}} = \frac{1}{\tau_{\rm rt}} - \int_{-K'}^{K'} d\epsilon' W(\epsilon') \quad (22)$$

with some given cutoff K' not further specified.

To understand the behavior of the inelastic relaxation time at small magnetic field one has to recall that the scattering processes at $B = 0$ are almost elastic, a typical energy transfer being smaller or of the order of the Korringa rate K. Thus, subtraction of the elastic processes leads to a drastic decrease of the inelastic relaxation rate, or to an increase of the inelastic relaxation time. For finite, small magnetic fields, however, the inelastic relaxation is of order $K + E_H$ and therefore will lead to an increase of order $(E_H/K)^2$. This term has to be compared with the monotonic decrease of order $(E_H/eU)^2$ and dominates in the regime $\rho J \ll 1$ explaining the increase of the inelastic relaxation rate for small magnetic fields.

A second way to discuss inelastic relaxation is to introduce the so-called energy relaxation time defined as an average energy-transfer rate. It is defined as

$$\frac{1}{\tau_\epsilon} \equiv -\frac{1}{\bar{\epsilon}} \int d\epsilon \rho(\epsilon) \epsilon I\{f\}. \quad (23)$$

Here $\rho(\epsilon)$ is the electron density of states, while $\bar{\epsilon}$ is a constant reference energy to normalize the particle energy. A natural scale for $\bar{\epsilon}$ at $eU \gg k_B T$ is eU. Since $eU \ll D$, where
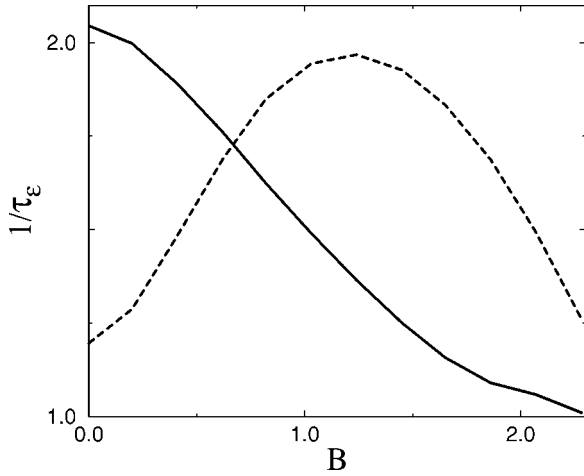
FIG. 4. Inverse energy relaxation time $1/\tau_\epsilon$ (solid line) in arbitrary units for $U=0.3$ mV depending on magnetic field B measured in Tesla. The dashed line shows the same quantity rescaled by 2/30 where all transferred energies ω in Eq. (24) are added positively.

D is the electronic bandwidth, the electron density of states can be regarded as energy independent, and after some algebra we get

$$\frac{1}{\tau_\epsilon} = -\frac{\rho}{\epsilon} \int d\epsilon \int d\omega W(\omega) \omega f(\epsilon)[1 - f(\epsilon - \omega)]. \quad (24)$$

One notices that this expression does not contain elastic scattering.

In Fig. 4 we show the magnetic-field dependence of the inverse energy relaxation time $1/\tau_\epsilon$ in arbitrary units for $U=0.3$ mV (solid line). We observe a monotonic decrease of the total energy transferred with increasing magnetic field. Note, that using the effective electron-electron interaction with a constant lifetime, meaning one fixes the lifetimes in the denominators of the Eqs. (9) and (10) at resonance, implies $1/\tau_\epsilon \equiv 0$ because of energy conservation. The dissipative motion of the spin system, however, virtually breaks energy conservation leading to a finite result. Considering Eq. (24) as the average $(\rho/\bar{\epsilon}) \int d\epsilon d\omega \ldots$ of the energy transfer, one finds in the integrand, depending on the energy, both positive and negative contributions. Although the average (24) monotonically decreases when B increases, the positive and negative contributions in fact increase for small magnetic fields $E_H \ll eU$. For comparison we show by the dashed line the average (24) where all transferred energies ω are added positively. This quantity, in contrast, shows the non-monotonic behavior in dependence of magnetic field. The physical relevance of this quantity, however, is not clear. This observation shows that the notion of a single energy relaxation time to describe energy relaxation is quite misleading. What happens is that nonequilibrium spins just *redistribute* the electron energy between different energy regions, the extra energy being transferred due to diffusion of "hot" electrons in real space.

In the experimental papers (Refs. 1,11, and 14), as well as in the theoretical ones based upon the t matrix approach (Refs. 6,7, and 10), a contribution of two-particle scattering

processes was also discussed. The results are expressed in terms of an effective interaction strength γ, which in our notation reads $\gamma = (\rho J)^2 / \tau_{sf}$. In the experimental papers, the results for $B=0$ and for finite magnetic fields were fitted assuming the same shape of the electron-electron interaction kernel $\propto 1/\omega^2$. According to our findings, the behavior of the interaction kernel differs from ω^{-2}. Consequently, it is difficult to compare their and our results.

B. Parameters obtained from experiment

Now let us briefly discuss the parameters obtained from the fit of the experimental data. Similarly to Ref. 7 where the first experiments[11] with Cu were fitted, we determine the Kondo temperature and the impurity density (see Sec. IV) from the distribution function at $B=0$. These values yield $T_K \approx 0.4$ K and $c_{imp} = 8$ ppm, respectively. The procedure proposed in Ref. 12, based on the analysis of the saturated phase breaking time, would suggest a Kondo temperature below $T \approx 0.1$ K, see also Ref. 13. However, assuming such a small T_K in our formalism, we would disagree with the experimentally observed distribution function at $B=0$ in Ref. 11. Here, we want to mention that we used the Kondo temperature in its simplest form based on the leading-logarithmic approximation. Corrections may still be large for this quantity and this disagreement could possibly be resolved using a refined version.

The procedure based on the estimate of the decoherence time τ_ϕ leads to some other inconsistencies. Namely, an estimation of the phase coherence time with our parameters would lead to $\tau_\phi \approx \tau_{sf}/2 \approx 0.06$ ns while, according to Ref. 12, $\tau_\phi \approx 1$ ns. In return, a fit of the decoherence time in Ref. 13 using the same τ_{sf} has lead to an impurity density of $c_{imp} \approx 0.15$ ppm much lower than our estimated impurity density. This means that using the standard theory of weak localization[26] the impurity spins should produce much higher decoherence rates than those observed experimentally. The main problem in comparing these two quantities may be the following: the decoherence time is measured in equilibrium and it saturates in the case of Cu below the Kondo temperature if we assume that both τ_ϕ and the energy relaxation are determined by the Kondo impurities. In that region, however, our treatment, as well as the standard theory of weak localization using the spins as random classical objects, become inaccurate. It is the aim of future work to develop a theory valid below T_K.

In our treatment we used some assumptions that were not addressed so far. First, we used the same distribution function for the electrons with different spin projections and the standard diffusive form of the Boltzmann equation. The latter assumption can be justified because the elastic relaxation time[14,25] $\tau_{imp} \approx 0.01$ ps is much smaller than that for inelastic scattering. The usage of a single distribution function is certainly fulfilled when the spin-orbit relaxation rate τ_{so}^{-1} is larger than the rate τ_{sf}^{-1} of processes that tend to violate the electron-spin symmetry. This assumption is supported by the results of the experiment[12] yielding $\tau_{so} \approx 39$ ps, whereas τ_{sf} is of the order of few nanoseconds.

We have disregarded some scattering mechanisms to focus on the magnetic dependence and to discuss the influence of this sort of impurities only. Direct electron-electron interaction leads to a pronounced smearing of the distribution function at low-energy transfer. That can be important at rather large magnetic fields when the energy relaxation mediated by magnetic impurities vanishes. Since this additional effect at $B=0$ is much weaker than the contribution by magnetic impurities, it cannot explain the deviations from experiment in the region of small-energy transfer. A comparison of the relaxation rates in Cu with realistic parameters has shown that the direct electron-electron interaction in the relevant frequency regime is about one order smaller than the corresponding effective interaction mediated by Kondo impurities.

In Appendix B we determine the renormalized coupling constant J that replaces the bare coupling constant J_0. The calculations are performed within a random-phase-like approximation. All higher-order corrections are supposed to be taken into account by the renormalization of the coupling constant J. This procedure, as known, leads to the so-called overcounting problem, which has been considered both for the electron[27] and pseudo-Fermion[28] self-energy. In these papers an attempt to cure this problem by setting the energy variable of the renormalized quantity to some special value has been made. No general method that would allow one to avoid the overcounting has been suggested so far. The only message is that as long as the renormalization is weak and the renormalized vertices are changing slowly with energy, one can use the "double dressed" vertices instead of the "single dressed" ones, using the language of Ref. 27. Here, we simply adopt this "rule," however, having in mind that if the renormalized quantities get too much structure, i.e., in the Kondo regime, this approach may become inaccurate. Our renormalized vertices are similar to those obtained using the Hamann approximation[29] in the *t*-matrix approach by Keiter,[30] which is a generalization of Suhl's dispersion approach[31] to finite magnetic fields. We further neglected the non-spin-flip contribution, which may be put into the free Hamiltonian and does not influence energy relaxation.

In the calculation of the correlation functions (9) and (10) we neglected the Knight shift as well as the frequency and Zeeman energy renormalizations. The Knight shift just leads to a simple addition to the "not really known" Zeeman splitting of the impurity spin and can be disregarded. The other terms can be determined by the Kramers-Kronig relation from the Korringa widths (12) and (13). They vanish for $\epsilon, E_H = 0$ and give just a renormalization of higher order in $(\rho J)^2$ which is usually disregarded well above the Kondo temperature. However, below the Kondo temperature these corrections would lead to an anomalous behavior and one has to go beyond the lowest order in the memory function even if one uses already renormalized coupling constants, see Ref. 28 for a discussion.

C. Kondo Temperature

The regime where all our calculations are actually valid is defined here as the regime where the lowest order in the logarithmic corrections, such as in Eqs. (B4) and (B5), are still small compared to 1. This is what we actually mean when speaking about a "non-equilibrium" regime or about a situation "above the Kondo temperature." The Kondo temperature is usually defined by the electron temperature where perturbation theory starts to fail. The terms of the perturbative expansion explicitly depend on the electron distribution function. As a result, even when the bath temperature is reduced below T_K, the perturbative approach can still be applied provided that the deviation from equilibrium is strong enough.

In Refs. 8, 9, and 10 the use of an effective spatially dependent Kondo temperature $T_K^*(x) = T_K^{1/x}/(eU)^{(1-x)/x}$ was proposed for electrons energetically near the Fermi point $\epsilon = -eU/2$ using the free solution (1) as a basis of the renormalization. For electrons near $\epsilon = eU/2$ one has simply to replace $x \to 1-x$. In these terms the effective Kondo temperature in the nonequilibrium situation is always smaller than the equilibrium Kondo temperature.

For an arbitrary distribution function it is not as straightforward to calculate the renormalized quantities as it is for the free solution (1). Equivalently to the notion of a renormalized Kondo temperature we propose to use a local temperature $T^*(x)$ describing the nonequilibrium situation. The Kondo temperature then equals its bulk equilibrium value and the local temperature is a spatially dependent functional of the distribution function. For strong electron-electron interaction or equivalently in the middle of a very long wire, $T^*(x)$ equals the analytically determined "hot electron" temperature[15,17,18] independent of the scattering mechanism. Further, this temperature fulfills the boundary conditions $T^*(x=0,1) = T_{\text{bath}}$. Therefore, at the ends of the wire and for temperatures explored experimentally, we are below Kondo temperature and our approach is inadequate. Here, we assume that the boundary regions where our approach fails are narrow and do not influence the distribution function in the middle of the wire. We believe that this assumption is fulfilled for long wires that were studied in experiments.[1,11,14] Further, it is obvious that our approach becomes more accurate for larger applied voltages when the distribution function at $B=0$ is a function of ϵ/eU only. This is the reason why we focus more on $U=0.3$ mV. It turns out (see below for details) that for $U=0.1$ mV and smaller voltages our theoretical approach reaches its limit of validity within the experimentally explored temperature range.

To be more specific, we give an analytic expression for the effective temperature in the case of weak smearing. The distribution function then equals the free solution (1) and the smearing is just included in an effective temperature T_{eff} characterizing the energetic width of the smeared steps. (Here, the Boltzmann constant k_B is set to one.) For example, one can determine T_{eff} as $T_{\text{eff}}(\epsilon, x) = -(1-x) \times [4 \partial f(\epsilon, x)/\partial \epsilon]^{-1}$ for $\epsilon \approx eU/2$. For simplicity we restrict ourselves to $B=0$, but the generalization is straightforward. As a basis of the renormalization we use Eqs. (B3) and (B5). Following the usual poor man's scaling procedure we get

$$\rho J(\epsilon) = \frac{\rho J_0}{1 - \rho J_0 g(\epsilon)}, \tag{25}$$

whereby we adiabatically integrated out all high-energy contributions from $-D$ to $\epsilon-\tilde{D}$ and D to $\epsilon+\tilde{D}$ letting $\tilde{D}$ to tend to zero. This procedure at finite temperature or finite effective temperature leads to an effective lower-energy cutoff which is either ϵ, $eU/2$, or T_{eff} and follows immediately from

$$g(\epsilon) \approx (1-x)\ln\left[\frac{D}{|\epsilon-eU/2|+T_{\text{eff}}}\right] + x\ln\left[\frac{D}{|\epsilon+eU/2|+T_{\text{eff}}}\right].$$
(26)

Inserted into Eq. (25), we get for the renormalized coupling constant

$$\rho J(\epsilon) = \ln\left[\frac{(|\epsilon-eU/2|+T_{\text{eff}})^{1-x}(|\epsilon+eU/2|+T_{\text{eff}})^x}{T_K}\right]^{-1}$$
(27)

with

$$T_K = De^{-1/\rho J_0}.$$
(28)

For sufficiently weak smearing $T_{\text{eff}} \ll eU$ mostly electrons near the Fermi points $\epsilon \approx \pm eU/2$ contribute. We may define a local temperature for electrons depending on the Fermi point. For electrons at $\epsilon \approx eU/2$, we get $T_+^*(x) = T_{\text{eff}}^{1-x}(eU)^x$. The other local temperature for electrons at $\epsilon \approx -eU/2$ reads $T_-^*(x) = T_{\text{eff}}^x(eU)^{1-x}$. Here, of course, the effective smearing T_{eff} depends on x and coincides at the ends of the wire ($x=0,1$) with the bath temperature T_{bath}. Since electrons of both Fermi points contribute to inelastic processes, one has to average the effective temperatures. The simplest average that yields the correct expression in the middle and at the ends of the wire reads $T^*(x) = (1-x)T_{\text{eff}}^{1-x}(eU)^x + xT_{\text{eff}}^x(eU)^{1-x}$, because at $x=0,1$ only electron at one Fermi point contributes.

In the middle of the wire, we get simply the requirement $T_{\text{eff}}eU \gg T_K^2$ for the calculations to be valid. If the smearing becomes stronger and T_{eff} is of the order of eU, or even larger, we get from Eq. (27) the requirement $T^* = T_{\text{eff}} \gg T_K$.

On the other hand, we may define an effective Kondo temperature by the failure of the perturbation theory. For electrons near the lower Fermi point $\epsilon \approx -eU/2$, we write

$$\rho J(\epsilon) = 1 \left/ x\ln\left[T_{\text{eff}}\frac{|eU|^{(1-x)/x}}{T_K^{1/x}}\right]\right.$$
(29)

and find the effective Kondo temperature to be $T_K^*(x) = T_K^{1/x}/(eU)^{(1-x)/x}$ as proposed in Ref. 10. The Kondo temperature for electrons near the upper Fermi point follows analogously. To our opinion the introduction of a local temperature is much more intuitive than a modification of the Kondo temperature. It seems to us that the latter concept can sometimes be misleading.

CONCLUSION

In this paper we studied energy relaxation mediated by magnetic impurities above Kondo temperature. We have shown that the effective electron-electron interaction is already included in the dissipative nature of the spin system. The finite linewidth in nonequilibrium proportional to the applied voltage leads to strong energy relaxation even for vanishing magnetic field where the spin states are degenerate. We succeeded in deriving a nonperturbative description valid for arbitrary magnetic fields where the perturbative t-matrix approach fails due to divergences in the two-electron scattering rates.

We characterized the efficiency of the energy relaxation by the slope of the distribution function at $\epsilon \approx 0$. The magnetic-field dependence of this quantity shown in Fig. 3 shows a nonmonotonic behavior. For small magnetic field, $E_H < eU/2$, the energy relaxation strength is increased and for larger magnetic fields, $E_H > eU/2$, it decreases again. Using the results in Sec. III we would even get a distribution function that depends on the pair of dimensionless energies ϵ/eU and E_H/eU only. These features meet qualitatively recent experimental data on energy relaxation in mesoscopic copper wires. Further, we found that the impurity spins are *out of equilibrium*. Namely, for $E_H < eU$ both spin states are occupied even at zero temperature, and the role of the effective temperature is played by the applied voltage. In this sense the impurity centers turn out to be "hot." Contrarily, when the magnetic field is strong, $E_H > eU$, i.e., only the lowest spin level should be occupied, the occupation of the "unfavorite" spin state is determined by high–order processes. Although the detailed comparison of the energy distribution functions fails to fit quantitatively all energy regions, this gives a strong indication that magnetic impurities are indeed responsible for energy relaxation in copper wires.

Several things remain to be done in order to achieve a quantitative description for the energy relaxation experiment in the broad regions of temperature and magnetic field. To go below the Kondo temperature, the overcounting problem has to be addressed. High-order corrections in impurity density might require a more complicated kinetic equation including quantum effects. Finally, for larger magnetic fields and/or low concentration of the localized spins, other relaxation mechanisms have to be accounted for.

To show that magnetic impurities are indeed present in copper wires, one has to describe all the available experiments using the same set of parameters. Since there are strong deviations from the magnetoresistance experiments, this is still an open question.

APPENDIX A: DERIVATION OF THE COLLISION INTEGRAL

We start with the "bare" Hamiltonian $H = H_0 + H_I$, where the free Hamiltonian is given in Eq. (7). In terms of pseudo-Fermions it reads
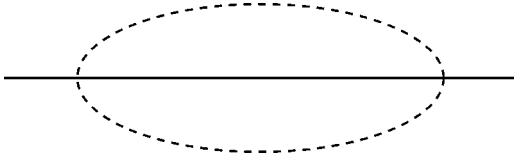
FIG. 5. Second-order self-energy graph for the electron Green's function

$$H_0 = \sum_{\mathbf{k}\sigma} \epsilon_{\mathbf{k}\sigma} C^\dagger_{\mathbf{k}\sigma} C_{\mathbf{k}\sigma} + \sum_\beta E_\beta a^\dagger_\beta a_\beta. \tag{A1}$$

Here the creation (annihilation) operators $C^\dagger_{k\sigma}$ ($C_{k\sigma}$) describe electrons while the operators $a^\dagger_\beta, a_\beta$ describe pseudo-Fermions. The pseudo-Fermion states are specified by $\beta = \pm$ having the energies $E_\pm = \mp g\mu_B B/2$. The interaction Hamiltonian

$$H_I = J_0 \sum_{\mathbf{k}\mathbf{k}'\sigma\sigma'} \mathbf{S}\cdot\mathbf{s}_{\sigma'\sigma} C^\dagger_{\mathbf{k}'\sigma'} C_{\mathbf{k}\sigma}$$

is the $s-d$ exchange Hamiltonian with the bare coupling J_0. Expressing spin operators through pseudo-Fermions, one can rewrite it as

$$H_I = \sum_{\mathbf{k}\mathbf{k}'} J^{\beta'\beta}_{\sigma'\sigma} C^\dagger_{\mathbf{k}'\sigma'} C_{\mathbf{k}\sigma} a^\dagger_{\beta'} a_\beta \tag{A2}$$

(summation over repeated indices is expected). In addition, we have to take into account the operator constraint $a^\dagger_+ a_+ + a^\dagger_- a_- = 1$ which can be formally done by a projection with the help of a complex chemical potential.[32]

Linear in the impurity density c_{imp}, the angular averaged collision integral for the classical Boltzmann equation can be expressed as[33,34]

$$I\{f\} = \frac{i}{\hbar}\{f(\epsilon)\Sigma^>(\epsilon) + [1-f(\epsilon)]\Sigma^<(\epsilon)\} \tag{A3}$$

with $\Sigma^{>/<}(\epsilon) = \Sigma_\sigma \Sigma^{>/<}(\mathbf{k}\sigma,\epsilon)/2$ where $\epsilon = \epsilon_{\mathbf{k}\sigma}$ is the spin averaged self-energy assumed to be independent of the angular momentum. $f(\epsilon)$ is the angular averaged distribution function for electrons of energy ϵ, where we suppressed the spatial dependence for convenience. Since the self-energy is proportional to the impurity density, we already replaced the electron Green's functions by their unperturbed form and integrated over frequency to get the classical form of the Boltzmann equation.

The electron self-energy in the lowest nonvanishing order, depicted in Fig. 5, is given by a pseudo-Fermion bubble and an electron or hole line inbetween,

$$\Sigma^>_2(\mathbf{k}\sigma,\epsilon) = c_{\mathrm{imp}} J^{\beta'\beta}_{\sigma'\sigma} J^{\beta\beta'}_{\sigma\sigma'} \sum_{\mathbf{k}'} \int \frac{d\omega}{2\pi}\frac{d\omega'}{2\pi} G^>_0(\mathbf{k}'\sigma',\epsilon-\omega')$$

$$\times \mathcal{G}^>_0(\beta',\omega+\omega')\mathcal{G}^<_0(\beta,\omega), \tag{A4}$$

where summation over internal spins is implied. The self-energy $\Sigma^<_2$ is given by the obvious change of the $<$ and $>$ signs in Eq. (A4). Since all corrections in the electron
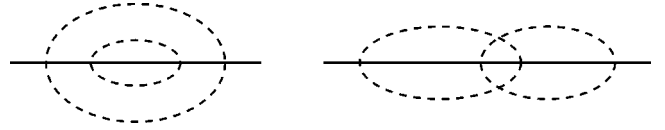

FIG. 6. Fourth-order graphs of second order in impurity density.

Green's functions are of higher orders in c_{imp}, they can always be used in the free form $G^<_0(\mathbf{k}\sigma,\omega) = 2\pi i f(\omega)\delta(\omega - \epsilon_{\mathbf{k}\sigma})$ and $G^>_0(\mathbf{k}\sigma,\omega) = -2\pi i[1-f(\omega)]\delta(\omega - \epsilon_{\mathbf{k}\sigma})$, respectively. The pseudo-Fermion Green's function in the lowest order reads $\mathcal{G}^<_0(\beta,\omega) = 2\pi i \mathcal{P}_\beta \delta(\omega - E_\beta)$ and has to be renormalized in the following. Note that when using the Abrikosov technique,[35] the occupation numbers $\mathcal{P}_\pm$ acquire an additional chemical potential $\exp(-i\lambda)$ and therefore $\mathcal{G}^>_0(\beta,\omega) = -2\pi i \delta(\omega - E_\beta)$, see Ref. 32. In contrast to Ref. 32 we assume that the occupation probabilities $\mathcal{P}_\pm$ are determined by the nonequilibrium electron distribution. Therefore they have to be found self-consistently.

For further proceeding, we have to classify the appearing graphs. Graphs including two pseudo-Fermion bubbles as shown in Fig. 6 are of second order in the impurity density and are therefore neglected. It is obvious that we may include an arbitrary number of additional electron-hole bubbles where each one is at least of order J_0^2. The two lowest-order graphs with one additional electron-hole bubble are depicted in Fig. 7. Considering only these two topologically different graphs in the self-energy, we obtain the t-matrix expression for the collision integral derived in Refs. 6 and 7, however, with bare coupling constants. The electron-hole pairs do not only renormalize the pseudo-Fermion propagator, which has been considered in Ref. 28, but also include bubbles connecting the upper and lower pseudo-Fermion lines. The latter graphs are so-called crossed diagrams and lead to vertex corrections[20] not included in a simple noncrossing approach.

All other corrections lead to higher orders in J_0 for a single electron-hole bubble or outer electron line. Above the Kondo temperature, it is conventionally accepted that one may write these corrections as a renormalization of the corresponding vertices and that in the leading logarithmic order the vertices are renormalized independently.[6,10] As a result, two dressed vertices instead of one are used. This procedure has been explicitly proven in the leading-logarithmic approximation both for the electron[27] and pseudo-Fermion[28] self-energies. An alternative derivation of the independent vertex renormalization has been given in Ref. 7.

Assuming this independent renormalization of vertices to be correct also for more involved graphs and that this renormalization depends only on the electron energies, one can equivalently start with a renormalized Hamiltonian restrict-
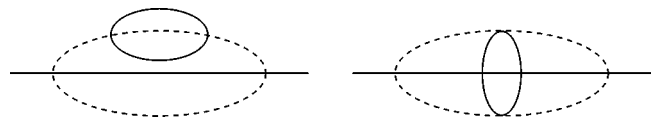

FIG. 7. Fourth-order self-energy terms including one additional electron-hole bubble.

ing the appearing graphs to simple electron-hole bubbles of the order of J^2 in the *renormalized* matrix elements $\tilde{J}^{\beta'\beta}_{\sigma'\sigma}$.

Neglecting the energy dependence of $\tilde{J}^{\beta'\beta}_{\sigma'\sigma}$ one obtains

$$\Sigma^>(\mathbf{k}\sigma,\omega) = c_{\text{imp}}\tilde{J}^{\beta'\beta}_{\sigma'\sigma}\tilde{J}^{\beta\beta'}_{\sigma\sigma'}\sum_{k'}\int\frac{d\omega'}{2\pi}\frac{d\hat{\omega}}{2\pi}$$

$$\times G_0^>(\mathbf{k}'\sigma',\omega-\omega')$$

$$\times\langle\mathcal{G}_0^>(\beta',\hat{\omega}+\omega')\mathcal{G}_0^<(\beta,\hat{\omega})\rangle_{\text{eh}}, \quad \text{(A5)}$$

where the average $\langle\cdots\rangle_{\text{eh}}$ means the dressing of the pseudo-Fermion bubble with all possible electron-hole pairs using renormalized coupling constants. Rephrasing the pseudo-Fermions in terms of spin operators and assuming isotropic coupling J, we may write

$$\Sigma^>(\omega) = -i\frac{c_{\text{imp}}}{4\rho}(\rho J)^2\int d\omega' C(\omega')[1-f(\omega-\omega')]$$
$$\text{(A6)}$$

with the time-dependent correlation function $C(t)$ given by Eqs. (5) and (6). The self-energy $\Sigma^<$ is given by the replacement $f\to 1-f$ and $C(\omega)\to C(-\omega)$, which is obvious since $C(t)$ is an autocorrelation function. Inserting this expression in Eq. (A3), we find the collision integral in the desired form (3). The spin-spin correlation functions are calculated then using a projection operator technique.[21] The actual procedure follows the lines outlined in Ref. 36 for the case of two-level systems.

APPENDIX B: VERTEX RENORMALIZATION

We proceed to determine the renormalized coupling constants. They can be derived in different ways: by a poor man's scaling procedure,[37] Suhl's t-matrix approach,[31] following Abrikosov and solving a generalized vertex equation,[35] or considering lower-order corrections and assuming similar resummation procedure as in equilibrium. According to Refs. 27 and 38 the renormalized vertex reads

$$\Gamma(\epsilon'\sigma',\omega'\beta'|\epsilon\sigma,\omega\beta) = \Gamma_0 + \Gamma_e(\epsilon+\omega) + \Gamma_h(\epsilon-\omega'),$$
$$\text{(B1)}$$

where

$$\Gamma_0 = J^{\beta'\beta}_{\sigma'\sigma} = J_0\mathbf{S}_{\beta'\beta}\cdot\mathbf{s}_{\sigma'\sigma} \quad \text{(B2)}$$

is the bare vertex of the $s-d$ exchange Hamiltonian. σ,β are the incoming electron and pseudo-Fermion spins and ϵ,ω are the incoming electron and pseudo-Fermion energies. The primed quantities are the outgoing spins and energies, respectively. Energy conservation is fulfilled at each vertex meaning $\epsilon'=\epsilon+\omega-\omega'$. The electron and hole vertex parts can be assumed to depend on a single energy variable.[28] The electron vertex Γ_e depends on the sum of incoming electron and pseudo-Fermion energies $\epsilon+\omega$, and the hole vertex part Γ_h depends on the difference of the incoming electron and outgoing pseudo-Fermion energies $\epsilon-\omega'$. In the lowest order in J_0 the retarded quantities read
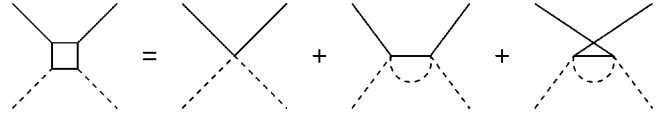

FIG. 8. Lowest-order vertex renormalization.

$$\Gamma^r_{e/h}(\epsilon) = \frac{i\rho J^{\beta'\gamma}_{\sigma'\kappa}J^{\gamma\beta}_{\kappa\sigma}}{2}\int\frac{d\xi}{2\pi}\int d\epsilon_{q\kappa}[G^r_0(q\kappa,\epsilon\mp\xi)\mathcal{G}^K_0(\gamma,\xi)$$

$$+G^K_0(q\kappa,\epsilon\mp\xi)\mathcal{G}^r_0(\gamma,\xi)] \approx J^{\beta'\gamma}_{\sigma'\kappa}J^{\gamma\beta}_{\kappa\sigma}\rho g(\epsilon\mp E_\gamma).$$

Here the upper sign stands for the electron vertex and the lower sign for the hole vertex, respectively. The auxiliary function

$$g(\epsilon) = \int_{-D}^{D}d\epsilon'\frac{f(\epsilon')-1/2}{\epsilon-\epsilon'+i\delta} \quad \text{(B3)}$$

leads in equilibrium to the usual logarithmic corrections.

Considering the lowest-order vertex corrections to the self-energy in Fig. 8 and assuming that the pseudo-Fermion energies are fixed to resonance, we get

$$\Gamma^\pm = \frac{J_0}{2}\left\{1+\frac{\rho J_0}{2}[g(\epsilon\pm E_H)+g(\epsilon)]\right\} \quad \text{(B4)}$$

for the spin-flip component proportional to $S^\pm$ and

$$\Gamma^z_\pm = (J_0/4)[1+\rho J_0 g(\epsilon\pm E_H)] \quad \text{(B5)}$$

for the component proportional to S^z applying to a spin-up (down) electron. This means that the leading renormalization of the "up" electron is given by the "down" electrons and vice versa. This anisotropic decomposition of the renormalized coupling constants has also been found by Keiter.[30] Setting the pseudo-Fermion energy to resonance is correct only for the lowest-order correction in the electron self-energy in Fig. 5. However, considering corrections to the graphs in Fig. 7, we find that there the pseudo-Fermion energies are weighted with a divergent term $\propto(\omega-E_\beta)^{-2}$ justifying the use of the resonance energy $\omega\approx E_\beta$ in the renormalization. Assuming that this is also justified for more involved graphs, we use these corrections as a basis of our renormalization. To write the renormalized Hamiltonian in terms of effective anisotropic and energy-dependent coupling constants, we reintroduce the spin operators and define $J^z_\pm(\epsilon)=4\Gamma^z_\pm(\epsilon)$ and $J^\pm(\epsilon)=2\Gamma^\pm(\epsilon)$.

To define a "Kondo scale" we consider the renormalized coupling constants as functions of the incoming electron energy and use the Hamann approximation[29] for the renormalized quantities. This approximation yields the same leading-logarithm expansion as the poor man's scaling procedure based on the expressions (B4) and (B5), however, taking care of the unitarity condition in each order. In this approximation, the S^z coupling constant reads

$$J^z_\pm(\epsilon)/J_0 = \{|1-(\pi\rho J_0)^2 S(S+1)/4-\rho J_0 g(\epsilon\mp E_H)|^2$$

$$+(\pi\rho J_0)^2 S(S+1)\}^{-1/2} \quad \text{(B6)}$$

in accordance with a high-temperature expansion of Keiter.[30] Analogously the spin-flip process renormalization reads

$$J^{\pm}(\epsilon)/J_0 = \{|1-(\pi\rho J_0)^2 S(S+1)/4$$
$$-\rho J_0[g(\epsilon)+g(\epsilon \pm E_H)]/2|^2$$
$$+(\pi\rho J_0)^2 S(S+1)\}^{-1/2}. \quad \text{(B7)}$$

These quantities coincide for $B=0$ with those used in Refs. 7 and 39 and cover the results obtained by the poor man's scaling procedure; see discussion about Kondo temperature in Sec. V. Note that the renormalized coupling constants remain finite also below the Kondo temperature where their meaning is questionable.

APPENDIX C: CALCULATION OF THE CORRELATION FUNCTION

We briefly present the method used to derive the results in Sec. III. Our main interest is the spin-spin correlation functions (6). Since $C(t)$ is an autocorrelator, its Fourier transform is given by the expression $C(\omega)=\tilde{C}(-i\omega+\delta)+\tilde{C}(-i\omega-\delta)$ where $\tilde{C}(z)$ is the Laplace transform of the correlator. Using projection operators $P^z X = S^z\langle XS^z\rangle/\langle S^z S^z\rangle$ for C_z and $P^{\pm}X = S^{\pm}\langle XS^{\mp}\rangle/\langle S^{\pm}S^{\mp}\rangle$ for the $C_{\pm}$ component, one can derive a formally exact integro-differential equation[21]

$$\dot{C}_a(t) = \Phi_a C_a(t) - \int_0^t du\,\phi_a(t-u)C_a(u) \quad \text{(C1)}$$

with the solution in terms of the Laplace transform

$$\tilde{C}_a(z) = \frac{C_a(t=0)}{z-\Phi_a+\tilde{\phi}_a(z)}, \quad \text{(C2)}$$

where $a=z,\pm$. Here $\Phi_z=\langle\dot{S}^z S^z\rangle/\langle S^z S^z\rangle=0$ and $\Phi_{\pm}=\langle\dot{S}^{\pm}S^{\mp}\rangle/\langle S^{\pm}S^{\mp}\rangle=\mp i\tilde{E}_H$ leads to the free propagation of the correlators, where $\tilde{E}_H$ includes the Knight shift neglected throughout the paper. The averages are calculated with the proper steady-state density defined by the stationary solution of the Boltzmann equation. The memory kernel $\phi_a(t)$ for the correlation function plays a similar role as the self-energy for the Green's function. For the $C_{\pm}$ term we find

$$\phi_{\pm}(t) = \frac{\langle\dot{S}_r^{\pm}(t)\dot{S}^{\mp}\rangle}{\langle S^{\pm}S^{\mp}\rangle} + \Phi_{\pm}\frac{\langle\dot{S}_r^{\pm}(t)S^{\mp}\rangle}{\langle S^{\pm}S^{\mp}\rangle}. \quad \text{(C3)}$$

Here the index r in $S_r^{\pm}(t)$ indicates that the dynamics of the spin operator is reduced by the projection. It is determined by the expression $\dot{S}_r^{\pm}(t) = \exp[i\hat{L}(1-P^{\pm})t]\dot{S}^{\pm}$ with the Liouville operator $\hat{L}$ acting as $\hat{L}\hat{X}=[H,\hat{X}]/\hbar$. The memory kernel for the C_z correlation function is simply given by Eq. (C3) with the replacement $\pm,\mp\to z$. Though formally exact, the above equations do not allow a simple calculation of the correlators. Here, we expand the kernel up to second order in the renormalized coupling J. Since the dynamics of the ex-

panded kernel function is oscillatory, the Fourier transformed correlation function has always the simple form

$$C_a(\omega) = \frac{2C_a(t=0)\text{Re}\,\phi_a(\omega)}{[\omega-i\Phi_a+\text{Im}\,\phi_a(\omega)]^2+[\text{Re}\,\phi_a(\omega)]^2} \quad \text{(C4)}$$

with $a=z,\pm$. Similar to Green's functions, this reflects the fact that in the steady state the retarded and advanced self-energies are complex conjugate, leading to a similar structure of the ">" or "<" Green's functions. Note that the roles of the imaginary and real parts of the memory kernel are opposite to those of the Green's functions because of different set of definitions. Further, we define $\text{Re}\,\phi_a(\omega)\equiv\text{Re}[\tilde{\phi}_a(-i\omega+\delta)]$ and the imaginary part $\text{Im}\,\phi_a(\omega)$ follows from a Kramers-Kronig relation. With $C_z(t=0)=\langle S^z S^z\rangle=1/4$ and $C_{\pm}(t=0)=\langle S^{\pm}S^{\mp}\rangle=\mathcal{P}_{\pm}$ and further neglecting the imaginary parts in the denominators, which lead to a frequency and Zeeman energy renormalization, we find the expressions (9) and (10) for the correlation functions.

APPENDIX D: DETAILED THEORETICAL DESCRIPTION

Starting with anisotropic and energy-dependent coupling constants derived in Appendix B, the interaction Hamiltonian in terms of impurity spin operators reads

$$H_I = \frac{1}{2}\sum_{kk'}\{S^+ J^+(\epsilon_{k\uparrow})C^\dagger_{k'\downarrow}C_{k\uparrow} + S^- J^-(\epsilon_{k\downarrow})C^\dagger_{k'\uparrow}C_{k\downarrow}$$
$$+ S^z[J^z_+(\epsilon_{k\uparrow})C^\dagger_{k'\uparrow}C_{k\uparrow} - J^z_-(\epsilon_{k\downarrow})C^\dagger_{k'\downarrow}C_{k\downarrow}]\}. \quad \text{(D1)}$$

Considering the electron self-energy in the Boltzmann equation the scattering rate W in the collision integral (3) depends on both, incoming electron energy ϵ and transferred energy ω

$$W(\epsilon,\omega) = (c_{\text{imp}}\rho/8\hbar)\{J^-(\epsilon)J^+(\epsilon')C_+(\omega)$$
$$+ J^+(\epsilon)J^-(\epsilon')C_-(\omega)+[J^z_+(\epsilon)J^z_+(\epsilon')$$
$$+ J^z_-(\epsilon)J^z_-(\epsilon')]C_z(\omega)\} \quad \text{(D2)}$$

with the outgoing electron energy $\epsilon'=\epsilon-\omega$; see Appendix A and Eqs. (5) and (6). The calculation of the correlation functions follows the lines in Appendix C and the general form (C4) leading the Eqs. (9) and (10) remain the same. The changes are only in the damping

$$\nu_z(\omega) = \pi\rho^2[\mathcal{P}_+\zeta_+(\omega-E_H)+\mathcal{P}_-\zeta_-(\omega+E_H)], \quad \text{(D3)}$$

$$\nu_{\pm}(\omega) = (\pi/4)\rho^2[\zeta_z(\omega\mp E_H)+\zeta_{\mp}(\omega)/\mathcal{P}_{\pm}], \quad \text{(D4)}$$

with the auxiliary functions

$$\zeta_z(\omega) = \int d\epsilon'[J^z_+(\epsilon')J^z_+(\omega+\epsilon')+J^z_-(\epsilon')J^z_-(\omega+\epsilon')]$$
$$\times f(\epsilon')[1-f(\omega+\epsilon')], \quad \text{(D5)}$$

$$\zeta_{\pm}(\omega) = \int d\epsilon' J^{\mp}(\epsilon')J^{\pm}(\omega+\epsilon')f(\epsilon')[1-f(\omega+\epsilon')]. \quad \text{(D6)}$$

The corresponding master equation (14) for the occupation probabilities $\mathcal{P}_\pm$ remains the same, but the rate changes to

$$\Gamma_\pm = \frac{\rho^2}{4\hbar\mathcal{P}_\pm} \int d\omega\, \zeta_\pm(-\omega) C_\pm(\omega). \tag{D7}$$

We used these formulas for the numerical determination of the distribution function in Sec. IV; however, the main features do not alter even if one uses the simplified description in Sec. III.

[1] F. Pierre *et al.,* in *Kondo Effect and Dephasing in Low-Dimensional Metallic Systems*, edited by V. Chandrasekhar, C. V. Haesendonck, and A. Zawadowski (Kluwer Academic, Dordrecht, 2001), pp. 119–132; e-print cond-mat/0012038.

[2] B. L. Altshuler and A. G. Aronov, in *Electron-Electron Interactions in Disordered Systems*, Vol. 10 of Modern Problems in Condensed Matter Sciences, edited by A. L. Efros and M. Pollak (North-Holland, New York, 1985), p. 1.

[3] P. Mohanty, E. M. Q. Jariwala, and R. A. Webb, Phys. Rev. Lett. **78**, 3366 (1997).

[4] P. Mohanty and R. A. Webb, Phys. Rev. Lett. **84**, 4481 (2000).

[5] J. Kroha, Adv. Solid State Phys. **40**, 267 (2000).

[6] A. Kaminski and L. I. Glazman, Phys. Rev. Lett. **86**, 2400 (2001).

[7] G. Göppert and H. Grabert, Phys. Rev. B **64**, 033301 (2001).

[8] J. Kroha, in *Kondo Effect and Dephasing in Low-Dimensional Metallic Systems* (Ref. 1), p. 245; e-print cond-mat/0102185.

[9] J. Kroha and A. Zawadowski, Phys. Rev. Lett. **88**, 176803 (2002).

[10] A. Zawadowski, e-print cond-mat/0105188.

[11] H. Pothier, S. Guéron, N. O. Birge, D. Esteve, and M. H. Devoret, Phys. Rev. Lett. **79**, 3490 (1997).

[12] A. B. Gougam, F. Pierre, H. Pothier, D. Esteve, and N. O. Birge, J. Low Temp. Phys. **118**, 447 (2000).

[13] F. Pierre, Ann. Phys. (Paris) **26**, 4 (2001).

[14] A. Anthore, F. Pierre, H. Pothier, D. Esteve, and M. H. Devoret, in *Electronic Correlations: From Meso- to Nano-Physics*, edited by T. Martin, G. Montambaux, and J. Tran Than Van (EDP Sciences, Paris, 2001), p. 301; e-print cond-mat/0109297.

[15] H. Pothier, S. Guéron, N. O. Birge, D. Esteve, and M. H. Devoret, Z. Phys. B: Condens. Matter **103**, 313 (1997).

[16] K. E. Nagaev, Phys. Lett. A **169**, 103 (1992).

[17] K. E. Nagaev, Phys. Rev. B **52**, 4740 (1995).

[18] V. I. Kozub and A. M. Rudin, Phys. Rev. B **52**, 7853 (1995).

[19] J. Korringa, Physica (Amsterdam) **XVI**, 601 (1950).

[20] P. Wölfle, W. Brenig, and W. Götze, Z. Phys. **235**, 59 (1970).

[21] H. Grabert, *Projection Operator Techniques in Nonequilibrium Statistical Mechanics* (Springer, New York, 1982).

[22] The *t*-matrix approach in Ref. 7 has been generalized to finite magnetic fields.

[23] C. Van Haesendonck, J. Vranken, and Y. Bruynseraede, Phys. Rev. Lett. **58**, 1968 (1987).

[24] W. Wöger and J. Zittartz, Z. Phys. **261**, 59 (1973).

[25] C. Kittel, *Introduction to Solid State Physics* (Wiley, New York, 1996).

[26] S. Chakravarty and A. Schmid, Phys. Rep. **140**, 193 (1986).

[27] S. D. Silverstein and C. B. Duke, Phys. Rev. **161**, 456 (1967).

[28] A. Zawadowski and P. Fazekas, Z. Phys. **226**, 235 (1969).

[29] D. R. Hamann, Phys. Rev. **158**, 570 (1967).

[30] H. Keiter, Z. Phys. B **23**, 37 (1976).

[31] H. Suhl, Phys. Rev. **138**, A515 (1965).

[32] N. S. Wingreen and Y. Meir, Phys. Rev. B **49**, 11 040 (1994).

[33] J. Rammer and H. Smith, Rev. Mod. Phys. **58**, 323 (1986).

[34] G. D. Mahan, *Many-Particle Physics* (Plenum, New York, 1993).

[35] A. A. Abrikosov, Physics (Long Island City, N.Y.) **2**, 21 (1965).

[36] H. Grabert and H. R. Schober, Appl. Phys. (N.Y.) **73**, 5 (1997).

[37] P. W. Anderson, J. Phys. C **3**, 2436 (1970).

[38] C. B. Duke and S. D. Silverstein, Phys. Rev. **161**, 456 (1967).

[39] W. Brenig, J. A. Gonzalez, W. Götze, and P. Wölfle, Z. Phys. **235**, 52 (1970).